Post-translational Covalent Labeling Reveals Heterogeneous Mobility of Individual G Protein-Coupled Receptors in Living Cells

Michael Prummer,[a] Bruno H. Meyer,[a, b]
Raphael Franzini,[a] Jean-Manuel Segura,[a]
Nathalie George,[a] Kai Johnsson,[a] and Horst Vogel*[a]

The lateral mobility of proteins and lipids in the cell membrane plays a central role in the transfer of information between and within cells in organisms. Thermally activated random movement is essential for bringing signaling partners into contact and allows for their subsequent dissociation, at no cost to metabolic energy. In contrast to earlier views,[1,2] the organization of the plasma membrane of living cells is highly heterogeneous and dynamic, which is essential for cellular functioning.[3–9] Observing the motion of single membrane proteins and lipids has allowed the investigation of their mutual interactions and the complex architecture of the plasma membrane in great detail.[10–14] In order to achieve single-molecule sensitivity and selectivity, markers, such as gold nanoparticles (~40 nm diameter), semiconductor quantum dots (~15 nm diameter), fluorescent proteins (~4 nm diameter), or organic fluorophores (~1.5 nm diameter)—which have been used here—have to be attached specifically to the protein of interest.

Current labeling strategies for single-molecule imaging of proteins in live cells involve the use of fluorescent analogues of i) ligands,[11, 15–18] ii) externally added proteins,[19–22] as well as iii) fusion to autofluorescent proteins.[12, 23–25] Each labeling technique has certain advantages and disadvantages. i) Receptor ligands can be coupled to diverse high-performance organic fluorophores but this is a cost and labor intensive process that requires a different synthesis strategy for each particular ligand. The conjugate often has substantially modified properties compared to the unlabeled ligand and only allows for the study of the ligand-bound state of the receptor. ii) Fluorescent antibodies are available for a broad range of proteins but they are often larger than the protein of interest and might interfere with its mobility and functionality. iii) Green fluorescent protein (GFP) and its variants can be attached genetically at different positions to the target protein in a 1:1 stoichiometry. However, GFP suffers from poor photostability,[12] the tendency to form oligomers,[26] and spectral overlap with other cellular luminescent compounds; this leads to substantial autofluorescence. Also, for the study of proteins in the plasma membrane it is preferable to only label the properly translocated fraction, especially in cases where this fraction is small.

Here, we demonstrate the advantages of a novel post-translational labeling technique for single-molecule imaging. We tracked individual unliganded G protein-coupled receptors (GPCRs) and thus determined their diffusion behavior on the plasma membrane of living cells. The labeling comprises enzymatic transfer of the phosphopantetheine of a fluorescent coenzyme A (CoA) conjugate to an acyl-carrier protein (ACP) fused to the target protein.[27] This technique enabled us to observe single GPCRs because several obstacles had been mastered: i) proteins not properly inserted in the plasma membrane were not labeled and hence did not contribute to out-of-focus background fluorescence; ii) the fraction of labeled protein could be precisely controlled; this ensured a low and well defined dye concentration required for single-molecule detection; and iii) long-wavelength dyes (Cy5) with high-absorption cross section, high quantum yield, and high photostability were used for an improved signal-to-background ratio and observation time; iv) nonspecific binding of the label to the plasma membrane, the most crucial obstacle, was reduced by the presence of the hydrophilic CoA moiety.

As a prototypic GPCR we investigated the neurokinin-1 receptor (NK1R) to which ACP was fused at the N terminus. NK1R mediates diverse processes in the human body, such as nociception, neural inflammation, or smooth muscle contraction, and therefore receives considerable attention as a drug target, for instance for treatment against depression.[28] We have previously shown that the ACP–NK1R fusion protein is activated by binding of its natural agonist, substance P (SP), at a similar effective concentration (EC_{50}) as the wild type.[29] Here we used ACP labeling to follow the mobility of single NK1Rs in live cells by using a home-built wide-field microscope. The low autofluorescence at the observation wavelength and the absence of labeled intracellular receptor enabled us to focus on receptors in the upper cell membrane where their motion is not influenced by the contact area of the cell with the supporting glass surface. With total internal-reflection microscopy one can achieve excellent contrast by illuminating only a thin section of up to a few hundred nanometers away from the glass surface. However, it is generally only possible to observe objects close to the lower membrane, which is in contact with the glass support. Figure 1 A shows a typical micrograph of isolated receptors (arrows) on the upper membrane of a HEK293 cell that stably expressed ACP–NK1R. While at the outer rim of the cell the high curvature leads to an increased out-of-focus fluorescence, on the flat inner part single NK1Rs are visible at a high signal-to-background ratio. Single-molecule trajectories were constructed by connecting corresponding spots in consecutive frames by using a custom-designed single-particle tracking (SPT) algorithm. The precision of position determination in our case was 35 nm (standard deviation measured for immobile molecules on the glass surface) and was limited by the number of detected photons from the molecule compared to the background level.

[a] Dr. M. Prummer, Dr. B. H. Meyer, R. Franzini, Dr. J.-M. Segura, Dr. N. George, Prof. K. Johnsson, Prof. H. Vogel
Institute of Chemical Sciences and Engineering
Ecole Polytechnique Fédérale de Lausanne (EPFL)
1015 Lausanne (Switzerland)
Fax: (+41) 21-693-6190
E-mail: horst.vogel@epfl.ch

[b] Dr. B. H. Meyer
Present address:
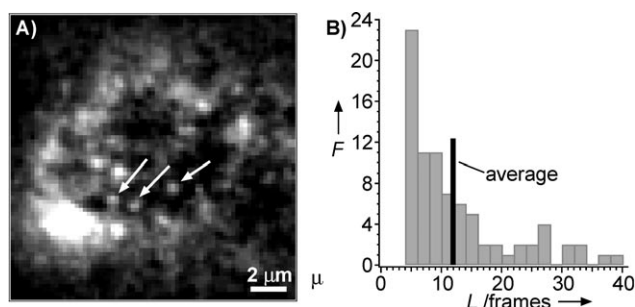Novartis Institutes for BioMedical Research
4002 Basel (Switzerland)

Figure 1. Tracking individual GPCRs on living cells. A) Fluorescence image of individual ACP–NK1Rs (arrows) in the upper membrane of a stably transfected HEK293 cell (see Experimental Section). Large areas of the image exhibited high background fluorescence, partly from clustered or out-of-focus receptors and were disregarded in the analysis. B) Frequency of the length, $F(L)$, of 80 traces of Cy5-labeled ACP–NK1R before photobleaching (50 ms illumination time, 10 Hz frame rate) with an average of 12 frames. Only traces longer than four frames were taken into account.

The ACP labeling scheme allows the use of any chromophore that can be coupled to CoA. The use of Cy5 resulted in a trace-length distribution with a relatively high average number of twelve detectable frames before photobleaching and a considerable fraction of molecules visible for more than 20 frames (Figure 1 B). Other near-infrared dyes, like Alexa647 delivered similar results. This number has to be compared to the 2–3 frames that are detectable on average when yellow fluorescent protein (YFP) is used as a label.[30] Avidin-functionalized semiconductor quantum dots and colloidal gold or latex nanoparticles could also be attached to ACP-modified membrane proteins with biotinylated CoA.[31] These would have the advantage of no or little photobleaching, but have the drawback of large sizes, intrinsic multivalency, and "stickiness". Depending on the preparation of quantum dots, frequent long dark states can render extended periods of tracking difficult.

Protein motion in cell membranes is characterized by the evolution of the two-dimensional mean-square displacement (MSD) as a function of time (t). Free diffusion exhibits a linear increase, $MSD(t) = 4Dt$; whereas diffusion within confined domains leads to $MSD(t) = L^2/3[1-\exp(-12Dt/L^2)]$; where L is the diameter of the domain and D the diffusion coefficient.[12] In single-particle tracking of dye molecules it is common practice to construct the probability distribution $P(r^2; t_{lag})$ for the occurrence of a square displacement smaller than r^2 for each time-lag (t_{lag}).[12] For molecules with identical (2D) diffusion behavior $P(r^2; t_{lag}) = 1-\exp(-r^2/4Dt_{lag})$, while the presence of several subpopulations leads to an equivalent expression containing the sum of weighted exponentials. This way, the composition of a mixed ensemble and the different diffusion coefficients can be retrieved from the collected recordings of many molecules, even if each individual trajectory is very short.

Figure 2 A shows the experimental cumulative probability distribution (black dots) of finding a molecule within a circle of radius, r, after seven observations (700 ms). It is remarkable that even the two-component model (dark gray dotted line) does not explain the data sufficiently well, as seen by the inhomogeneity of the residuals; a three-component model (light
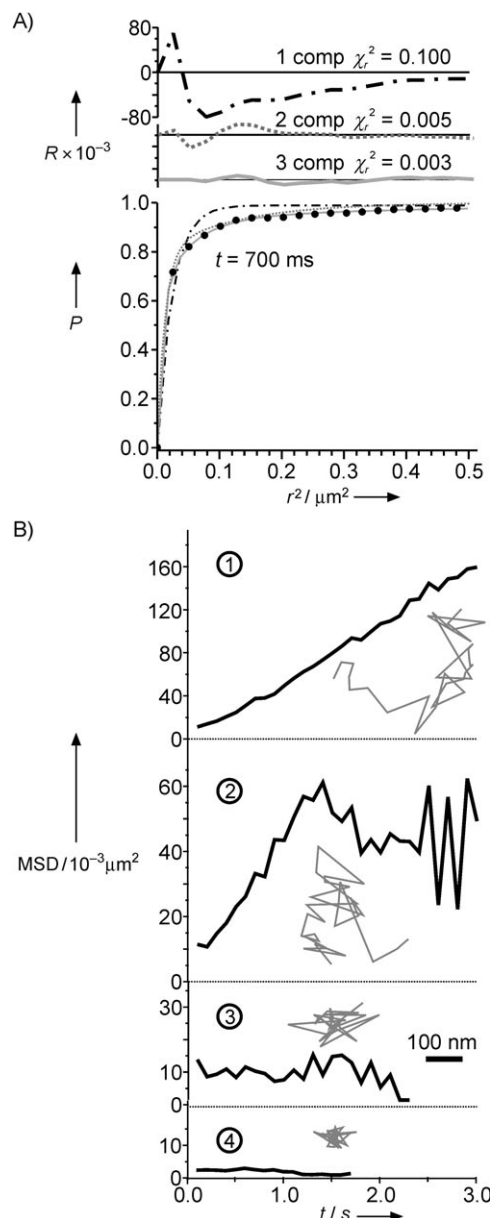

Figure 2. Mobility analysis of single unliganded NK1Rs. A) Cumulative probability distribution, $P(r^2)$, for finding the receptor within a circle of radius r after seven consecutive observations. The experimental distribution (●) was fitted with the analytic expression for 1 (–•–•), 2 (dark gray dotted line), and 3 components (light gray full line) with the residuals R of the fit. B) Examples of single-molecule trajectories (gray) and their mean-square displacement time courses, $MSD(t)$ (black). The scale bar refers to the trajectories. The different classes are, graph 1: free Brownian motion; graph 2: confined motion; graph 3: strongly confined motion; graph 4: immobile.

gray full line) cannot be fitted with appropriate accuracy due to the large number of free parameters. This result reveals a very heterogeneous ensemble of NK1Rs, which cannot be investigated adequately by using averaging methods. Instead, it is necessary to analyze the diffusion of each particle independently and detect and discriminate different classes directly by considering the distribution of the individual behavior—a procedure which requires the recording of long trajectories.

Examples of different mobility classes of NK1R in HEK cells are depicted in Figure 2B (trajectories in gray, MSD(*t*) in black). Immobile molecules (graph 4) show a time-independent MSD with a magnitude similar to immobile dye molecules on a glass surface. Some molecules apparently diffuse within small (graph 3) or large domains (graph 2) while several exhibit free Brownian motion on a time scale of several seconds (graph 1). This heterogeneity is reflected in the distribution of initial diffusion coefficients, D_{1-3} (Figure 3, black full line), which spans
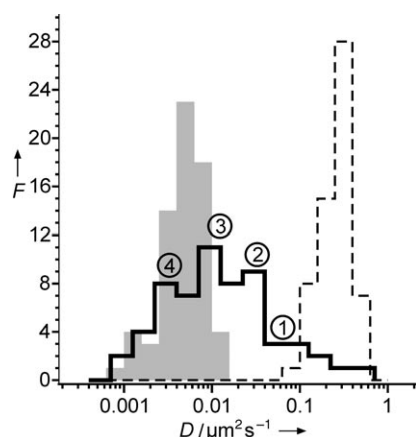

Figure 3. Histograms of the initial diffusion coefficients, D_{1-3}. The frequency, $F(D)$, of unliganded NK1Rs (black line) resulting from the analysis of 80 molecules, which contained about 1000 individual displacements, was compared to the distribution of fluorophores immobilized on a glass surface (gray area) and also simulated particles freely diffusing with $D = 0.3 \ \mu m^2 s^{-1}$ (----). The numbers indicate the location of the diffusion coefficient of the four examples specified in Figure 2.

three orders of magnitude from 0.0007 to 0.7 $\mu m^2 s^{-1}$. D_{1-3} is determined from the initial slope of the first three data points of MSD(*t*),[25] assuming that MSD(0) = 0. Comparison with immobile molecules (Figure 3, gray area) allows for the accurate assignment of NK1 receptors with $D_{1-3} < 0.01 \ \mu m^2 s^{-1}$ as being immobile. The mobile fraction of NK1R is widely distributed, and ranges from a rather slow part ($0.01 < D_{1-3} < 0.04 \ \mu m^2 s^{-1}$) to a population of relatively fast receptors ($0.07 < D_{1-3} < 0.7 \ \mu m^2 s^{-1}$). Simulated freely diffusing particles ($D = 0.3 \ \mu m^2 s^{-1}$) under similar conditions as in the experiment have a much narrower distribution (Figure 3, dashed line) and cannot account for the experimental observation.

Such heterogeneous diffusion properties are by far not a general feature of membrane receptors. In clear contrast, for instance, the MHC class II molecule was found to exhibit homogeneous free Brownian motion.[11] SPT on another GPCR, the μ-opioid receptor, revealed diffusion properties that were distinct from NK1R with either free hop-diffusion[25] or a slow motion of unconfined receptors,[6] depending on the preparation procedure. The metabotropic-glutamate receptor on the other hand showed heterogeneous diffusion with confined and free fractions—similar to NK1R—which was related to the existence of clusters of receptors with a scaffolding protein.[32]

The heterogeneous mobility of NK1R can have several origins: i) partitioning of the receptor inside membrane microdo-

mains[34] or clathrin-coated pits;[35] ii) interaction of the receptor with other membrane and cytosolic proteins, like hetero-trimeric G-protein and other direct effectors of GPCRs;[32,36] iii) direct or indirect interaction with the cytoskeleton.[25] A recent single-molecule study[17] revealed that application of the NK1R agonist, SP, leads to a decrease of the diffusion coefficient of NK1R which might correspond to modulation of the distribution described here. While the mechanism causing this mobility decrease is unknown, our data show that the involved interaction or confinement is already present in the absence of ligand since we observe a large fraction of immobile and confined molecules. Therefore, the agonist does not induce an interaction of the free receptor to particular proteins or confinement to newly formed compartments, but does rather modulate existing interactions.

In conclusion, we have demonstrated the power of ACP-mediated labeling of membrane proteins with organic dyes for single-molecule investigations on living cells by tracking of individual NK1Rs. Using highly photostable and bright organic fluorophores, we could precisely control the amount of labeled receptor and record long single-molecule trajectories with very high accuracy. In this way, we discovered a heterogeneous mobility distribution of a prototypical member of the GPCR superfamily. As ACP labeling is universally applicable to any membrane protein, we are confident that it will give a new pace to single-molecule live-cell experiments, complementary to other orthogonal labeling techniques.[37,38]

Experimental Section

Cell culture and labeling experiments: Adherent HEK293 cells that stably expressed ACP–NK1R (about 25000 receptors per cell) were generated from transiently transfected cells by selection with hygromycin B (200 $\mu g\,mL^{-1}$) and cultured as described.[29] Cells were grown in Dulbecco's modified Eagle's medium (DMEM) supplemented with fetal calf serum (FCS, 2.5%). The culture was kept at 37 °C in a humidified atmosphere with CO_2 (5%). For single-molecule imaging HEK293 cells were seeded two days before the experiment into six-well plates that contained glass cover slips (0.17 mm thick, 25 mm diameter) and DMEM/FCS (2 mL). Synthesis of CoA–Cy5 substrates and purification of phosphopantetheine transferase (AcpS from *E. coli*) was described previously.[27] Before labeling, the cells were washed once with PBS buffer. Labeling was performed by incubating the cells for 30 min at room temperature in PBS with $MgCl_2$ (10 mM), AcpS (1 μM), and CoA–Cy5 (50 nM). After incubation and prior to the experiment the cells were washed five times with PBS. When no enzyme was present virtually no unspecific binding was observed even after incubation of the cells for 30 min at concentrations of up to 5 μM CoA–Cy5 (data not shown).

All experiments were performed at room temperature. NK1Rs were able to activate the G_q-coupled signaling cascade and elicit calcium signaling at 25 °C.[29] HEK293T cells were kept at 37 °C in PBS for an extended period of time, rounded, and detached rapidly from the substrate, which inhibited tracking measurements.

Single-molecule wide-field microscopy: This was performed on a home-built setup.[18] A 633 nm HeNe laser (~1 mW) was used to illuminated a 15 μm diameter area. Fluorescence was collected with a 63x/1.2NA water immersion objective (Zeiss) and guided to an in-

tensified CCD camera (Pentamax, Roper Scientific, Tucson, Arizona) through appropriate filters. The question of whether each bright spot corresponded to a single NK1R was addressed by commonly accepted criteria; that is: i) the intensity was typical for single dye molecules, ii) it exhibited occasional blinking and dropped to background level in a single sharp step, and iii) the size and shape of the spot were diffraction limited.

Accompanying the experimental investigation, Brownian dynamics simulations were performed as a control to compare the mobility of NK1R with pure two-dimensional free diffusion. The custom Monte-Carlo algorithm utilized normal distributed microscopic displacements following $<r^2> = 4Dt$ from the random number generator implemented in Igor Pro (Wavemetrics, Lake Oswego, Oregon).

Acknowledgements

[1] S. J. Singer, G. L. Nicolson, *Science* **1972**, *175*, 720.
[2] P. G. Saffman, M. Delbrück, *Proc. Natl. Acad. Sci. USA* **1975**, *72*, 3111.
[3] K. Jacobson, E. D. Sheets, R. Simson, *Science* **1995**, *268*, 1441.
[4] K. Simons, E. Ikonen, *Nature* **1997**, *387*, 569.
[5] A. Pralle, P. Keller, E. L. Florin, K. Simons, J. K. Horber, *J. Cell Biol.* **2000**, *148*, 997.
[6] F. Daumas, N. Destainville, C. Millot, A. Lopez, D. Dean, L. Salome, *Biophys. J.* **2003**, *84*, 356.
[7] K. Ritchie, R. Iino, T. Fujiwara, K. Murase, A. Kusumi, *Mol. Membr. Biol.* **2003**, *20*, 13.
[8] K. Simons, W. L. Vaz, *Annu. Rev. Biophys. Biomol. Struct.* **2004**, *33*, 269.
[9] A. D. Douglass, R. D. Vale, *Cell* **2005**, *121*, 937.
[10] G. J. Schutz, G. Kada, V. P. Pastushenko, H. Schindler, *EMBO J.* **2000**, *19*, 892.
[11] M. Vrljic, S. Y. Nishimura, S. Brasselet, W. E. Moerner, H. M. McConnell, *Biophys. J.* **2002**, *83*, 2681.
[12] P. H. Lommerse, G. A. Blab, L. Cognet, G. S. Harms, B. E. Snaar-Jagalska, H. P. Spaink, T. Schmidt, *Biophys. J.* **2004**, *86*, 609.
[13] A. Kusumi, C. Nakada, K. Ritchie, K. Murase, K. Suzuki, H. Murakoshi, R. S. Kasai, J. Kondo, T. Fujiwara, *Annu. Rev. Biophys. Biomol. Struct.* **2005**, *34*, 351.
[14] K. Ritchie, X. Y. Shan, J. Kondo, K. Iwasawa, T. Fujiwara, A. Kusumi, *Biophys. J.* **2005**, *88*, 2266.
[15] Y. Sako, S. Minoghchi, T. Yanagida, *Nat. Cell Biol.* **2000**, *2*, 168.
[16] M. Ueda, Y. Sako, T. Tanaka, P. Devreotes, T. Yanagida, *Science* **2001**, *294*, 864.
[17] Y. Lill, K. L. Martinez, M. A. Lill, B. H. Meyer, H. Vogel, B. Hecht, *ChemPhysChem* **2005**, *6*, 1633.
[18] C. Schreiter, M. Gjoni, R. Hovius, K. L. Martinez, J. M. Segura, H. Vogel, *ChemBioChem* **2005**, *6*, 2187.
[19] V. T. Nguyen, Y. Kamio, H. Higuchi, *EMBO J.* **2003**, *22*, 4968.
[20] C. Nakada, K. Ritchie, Y. Oba, M. Nakamura, Y. Hotta, R. Iino, R. S. Kasai, K. Yamaguchi, T. Fujiwara, A. Kusumi, *Nat. Cell Biol.* **2003**, *5*, 626.
[21] L. Groc, M. Heine, L. Cognet, K. Brickley, F. A. Stephenson, B. Lounis, D. Choquet, *Nat. Neurosci.* **2004**, *7*, 695.
[22] U. Kubitscheck, D. Grunwald, A. Hoekstra, D. Rohleder, T. Kues, J. P. Siebrasse, R. Peters, *J. Cell Biol.* **2005**, *168*, 233.
[23] G. S. Harms, L. Cognet, P. H. Lommerse, G. A. Blab, H. Kahr, R. Gamsjager, H. P. Spaink, N. M. Soldatov, C. Romanin, T. Schmidt, *Biophys. J.* **2001**, *81*, 2639.
[24] T. Kues, R. Peters, U. Kubitscheck, *Biophys. J.* **2001**, *80*, 2954.
[25] K. Suzuki, K. Ritchie, E. Kajikawa, T. Fujiwara, A. Kusumi, *Biophys. J.* **2005**, *88*, 3659.
[26] D. A. Zacharias, J. D. Violin, A. C. Newton, R. Y. Tsien, *Science* **2002**, *296*, 913.
[27] N. George, H. Pick, H. Vogel, N. Johnsson, K. Johnsson, *J. Am. Chem. Soc.* **2004**, *126*, 8896.
[28] S. C. Stout, M. J. Owens, C. B. Nemeroff, *Annu. Rev. Pharmacol. Toxicol.* **2001**, *41*, 877.
[29] B. H. Meyer, K. L. Martinez, J.-M. Segura, P. Pascal, R. Hovius, N. George, K. Johnsson, H. Vogel, *FEBS Lett.* **2006**, *580*, 1658.
[30] G. A. Blab, PhD thesis, University of Leiden (The Netherlands), **2004**.
[31] N. Johnsson, N. George, K. Johnsson, *ChemBioChem* **2005**, *6*, 47.
[32] A. Serge, L. Fourgeaud, A. Hemar, D. Choquet, *J. Neurosci.* **2002**, *22*, 3910.
[33] K. Monastyrskaya, A. Hostettler, S. Buergi, A. Draeger, *J. Biol. Chem.* **2005**, *280*, 7135.
[34] B. H. Meyer, J.-M. Segura, K. L. Martinez, R. Hovius, N. George, K. Johnsson, H. Vogel, *Proc. Natl. Acad. Sci. USA* **2006**, *103*, 2138.
[35] L. Cezanne, S. Lecat, B. Lagane, C. Millot, J. Y. Vollmer, H. Matthes, J. L. Galzi, A. Lopez, *J. Biol. Chem.* **2004**, *279*, 45057.
[36] A. Pramanik, M. Olsson, U. Langel, T. Bartfai, R. Rigler, *Biochemistry* **2001**, *40*, 10839.
[37] E. G. Guignet, R. Hovius, H. Vogel, *Nat. Biotechnol.* **2004**, *22*, 440.
[38] J. Yin, A. J. Lin, P. D. Buckett, M. Wessling-Resnick, D. E. Golan, C. T. Walsh, *Chem. Biol.* **2005**, *12*, 999.